Optical Fiber Technology 30 (2016) 116–124

Contents lists available at ScienceDirect

Optical Fiber Technology

www.elsevier.com/locate/yofte

Regular Articles

Efficient routing and spectrum assignment in elastic optical networks with time scheduled traffic

Yang Qiu [a,*], Zheyu Fan [b], Chun-Kit Chan [b]

[a] College of Electrical & Information Engineering, Southwest University for Nationalities, Chengdu, China
[b] Department of Information Engineering, The Chinese University of Hong Kong, Hong Kong Special Administrative Region

ARTICLE INFO

Article history:
Received 27 October 2015
Revised 16 April 2016
Accepted 25 April 2016

Keywords:
Elastic optical networks
Routing and spectrum assignment
Spectrum efficiency
Time scheduled traffic

ABSTRACT

Elastic optical networks (EONs) employ dynamic routing and spectrum assignment (RSA) algorithms to support diverse services and heterogeneous requests. However, these RSA algorithms may possibly induce spectrum fragments when allocating spectrum to accommodate different service requests. Therefore, such induced spectrum fragments should also be regarded as spectrum consumption besides the allocated spectrum by RSA algorithms. In this paper, by additionally considering the holding times of lightpaths and service connections, we first introduce a comprehensive spectrum consumption model to simultaneously investigate both the allocated and the fragmented spectrum consumptions. Then we solve this model in both static and dynamic traffic scenarios, by either formulating the RSA problem with time-scheduled traffic or introducing a time-aware spectrum-efficient heuristics algorithm. Since no defragmentation is executed in spectrum allocation, the proposed RSA algorithm requires no traffic disruption and can be realized more easily in reality. Simulation results show that the proposed algorithm reduces the comprehensive spectrum consumption and has lower bandwidth blocking probability than the typical first-fit RSA algorithm.

1. Introduction

Elastic optical networks (EONs) have attracted much attention ever since they were first proposed due to their obvious advantage in spectrum provisioning [1]. Different from traditional wave length-division-multiplexing (WDM) [2] and multi-granularity grooming optical networks [3,4], EONs employ a finer spectrum allocation granularity, known as frequency slot (FS), and are able to assign spectrum to different services adaptively according to their bandwidth requirements with variable number of contiguous FSs. Thanks to the finer granularity, FS, employed in spectrum assignment, the flexibility of spectrum allocation and the efficiency of resource utilization have been remarkably improved, although it may also require some expensive components, such as bandwidth-variable optical cross-connects [5]. But their high cost may be reduced with the development and maturity of optical integration and wavelength selective switch technologies. Therefore, elastic optical networks are now considered a promising candidate solution to the next-generation high-speed optical networks.

Routing and spectrum assignment (RSA) algorithm [6], which seeks a transmission path for a service request and assigns spectrum on the sought path to the service, is the key enabling technology to realize dynamic spectrum allocation in elastic optical networks. Therefore, various RSA schemes for EONs [7–9], have been proposed recently, including the shortest path routing and first-fit spectrum allocation algorithm [7], and the distance-adaptive modulation formats allocation algorithms [8,9]. However, if a spectrum band is successfully assigned to a service by the aforementioned RSA algorithms, the assigned spectrum band cannot be re-used or changed on the transmission path, until the service expires. This is known as spectrum continuity constraints. Since practical networks always have limited capacity of spectrum conversion due to its high complexity and cost, this continuity constraint may induce spectrum fragmentation in network evolutions, connection tear-down operations, or some network maintenance procedures. Besides the spectrum continuity constraint, spectrum contiguity constraint is another important constraint in spectrum assignment, which requires that the spectrum band assigned to one service should be composed of multiple contiguous FSs. But such spectrum contiguous constraint may possibly leave some tiny spectrum fragments due to the finer spectrum granularity, FS, employed in spectrum assignment. If such tiny fragments are

* Corresponding author.
E-mail addresses: jimq2008@163.com (Y. Qiu), fz012@ie.cuhk.edu.hk (Z. Fan).

http://dx.doi.org/10.1016/j.yofte.2016.04.011
1068-5200/

accumulated before being properly handled, the available spectrum resource decreases and the networking performance deteriorates, because these tiny fragments cannot be used by any kind of services. Therefore, spectrum fragmentation [10,11] has become a serious issue in EONs and many schemes, known as defragmentation, have been proposed on it [12–22]. A make-before-break rerouting algorithm was proposed in [12] to reduce the generated spectrum fragments by rerouting the lightpaths for the existing services, but extra free spectrum and multiplexer/de-multiplexer may be required to create an alternative lightpath. In [13–17], spectrum retuning based algorithms were proposed to reduce the generated fragments in time-varying traffic, employing either spectrum expansion, contraction, reallocation policies [13–16], or hot-tuning technique [17]. Defragmentation algorithms with both rerouting and retuning were proposed in [18,19]. Although these defragmentation algorithms can successfully reduce the generated spectrum fragments by re-optimizing the spectrum resource, the traffic of the existing services may possibly be disrupted in lightpath rerouting or spectrum retuning procedures, which may lead to a large mount of loss in data and business, especially in high-speed transmissions. Regarding such traffic disruption in spectrum defragmentation, an auxiliary graph and maximum independent sets were introduced into spectrum retuning to minimize the traffic disruption [20,21]. In [22,17], defragmentation algorithms employing push–pull technique were proposed to avoid traffic disruption. However, in order not to disrupt the traffic, the whole spectral band in the spectrum retuning range is required vacant in push–pull technique to guarantee non-disruptive spectrum shifting. For instance, if the allocated spectrum of a service connection (assuming the service connection requiring one FS) is to be retuned from FS_m to FS_n (m and n are the indices of the FSs on a fiber link) by the push–pull defragmentation algorithm, all the FSs between FS_m and FS_n (including FS_n) need to be vacant for spectrum shifting in push–pull technique. If any FS between FS_m and FS_n is occupied, it should be shifted to the spectrum outside the band from FS_m to FS_n by the same technique (push–pull technique) so as to create the vacant spectrum band from FS_m to FS_n. This requires that there should have enough vacant spectrum outside the spectrum band from FS_m to FS_n on the fiber link for the occupied FSs between FS_m and FS_n. And this additional requirement for spectrum will reduce the successful probability of spectrum shifting in push–pull technique and thus reduces its effectiveness. In addition, fast tunable lasers are always needed for spectrum shifting in push–pull technique, which may increase the cost and the complexity of the system. In [23,24], fragmentation-aware spectrum assignment algorithms were introduced into EONs to solve spectrum fragmentation problem. By employing the parameter "cut" to calculate the number of spectrum blocks a provisioning scheme would break, fragmentation-aware algorithms increased the number of contiguous FSs in available spectrum bands when choosing the provisioning scheme with the least or no broken spectrum blocks. However, even with no broken spectrum blocks, an available spectrum band should be recognized as fragments if it had no enough contiguous FSs for any kind of services.

Previous investigations on RSA algorithms are focus on the allocated spectrum resources or the generated spectrum fragments. But, actually, both the allocated spectrum and the generated fragments are the spectrum consumption to accommodate service connections. Therefore, the two kinds of spectrum consumptions should be comprehensively considered in RSA algorithms, although they have different timing characteristics (i.e., the timing characteristics of the allocation spectrum depends on the holding-time of its served service connection, while the timing characteristics of the generated fragments depends on the adjacent allocated spectrum). In this paper, with the additional consideration of the holding times of lightpaths and connection requests, we introduce a comprehensive spectrum consumption model to simultaneously investigate both the allocated and the fragmented spectrum consumptions, and then try to solve this model in both static and dynamic traffic scenarios. In static case, in which all connection requests with their setup and tear-down times are known in advance, we formulate the RSA problem with time-scheduled traffic via Integer Linear Programming (ILP) to minimize the comprehensive spectrum consumption. In dynamic case, we propose a time-aware spectrum-efficient heuristics algorithm which takes the holding time of a new arrival connection request and the remaining holding time of existing lightpaths into consideration to minimize the comprehensive spectrum consumption. Simulation results show that the proposed algorithm can reduce the comprehensive spectrum consumption with no traffic disruption, while having lower bandwidth blocking probability than the typical first-fit RSA algorithm.

The rest of the paper is organized as follows. In Section 2, we introduce the comprehensive spectrum consumption model to simultaneously investigate both the allocated and fragmented spectrum consumptions. In Section 3, the ILP formulation for the RSA problem with time-scheduled traffic is introduced to solve the comprehensive spectrum consumption model in static traffic scenario. In Section 4, a time-aware spectrum-efficient heuristics algorithm is proposed to solve the comprehensive spectrum consumption model in dynamic traffic scenario. In Section 5, simulation results are presented to compare the performance of different RSA algorithms. Section 6 concludes this paper.

2. Comprehensive spectrum consumption model

In this section, a comprehensive spectrum consumption model is introduced to characterize both the allocated spectrum and the fragmented spectrum, via additionally considering the holding times of lightpaths and service connections. Although distance-adaptive modulation format allocation can further improve the spectral utilization efficiency by choosing more effective modulation format according to the transmission distance, bandwidth variable transponders are usually required in these systems to generate a large set of modulation formats and vary data-, symbol-, and code-rate according to actual traffic conditions [25]. Therefore, bandwidth variable transponders always require high-quality components and advanced DSP to meet the requirements of different modulation formats (MF) and transmission reach. In addition, bandwidth variable transponders may require multiple carriers (which can be realized by multiple lasers or subcarrier generation) for very high-rate transmissions [26]. All these may increase the cost and the complexity of a bandwidth variable transponder, especially for future ultra high-speed service connections. Thus, in this model, we use determined MFs for different kinds of service connections instead of considering distance-adaptive modulation format allocation, and the elasticity of the network is mainly from the used flex-grid switches in the network. As for the MF selection, we use the MF with low spectral efficiency for the current frequently-used low-speed service connections (e.g. 100 Gb/s) to meet the requirement of long transmission reach and system complexity, since these service connections have higher possibility to be requested in the whole network and are quite sensitive to the transmission reach and system complexity. But for the future ultra high-speed service connections (e.g. 1 Tb/s), the MF with high spectral efficiency is employed for them, since they are more bandwidth-hungry than the low-speed service connections. Considering the limited transmission range for different MFs and the existing physical impairments (e.g. transmission loss, dispersion and nonlinear impairments) in reality, we assume that optical amplifiers (e.g. EDFA) and some novel techniques (such as digital backpropagation (BP) [27], pilot-tone-based phase noise compensation [28], time-domain hybrid QAM [29], soft decision low-density parity-check (LDPC) codes [30], bit-interleaved coded modulation (BICM) [31]) can be used in the network to compensate physical impairments or increase the tolerance to physical impairments, which can effectively increase the transmission range for the MFs with high spectral efficiency. As discussed above, different kinds of service connections require unique spectrum bandwidth by employing different MFs, and the spectrum fragments can be defined as isolated bandwidth blocks without enough continuous FSs for any kinds of services. Since the comprehensive spectrum consumption is comprised of the allocated and the fragmented spectrum consumptions, each of which has a linear dependence with the spectrum bandwidth and its corresponding time information, it can be represented as

$$C_{\text{total}} = B_{\text{allocated}} \times T_{\text{allocated}} + B_{\text{fragment}} \times T_{\text{fragment}} \tag{1}$$

where C_{total} is the comprehensive spectrum consumption; $B_{\text{allocated}}$ and $T_{\text{allocated}}$ are the bandwidth and the holding time of the allocated spectrum, respectively; B_{fragment} and T_{fragment} are the bandwidth and the holding time of the fragmented spectrum, respectively. And we sum all these over connections, voids and links. In order to calculate C_{total} in Eq. (1), we employ $r(s, d, b_r, t_s, t_d)$ to represent a service connection request, where s and d denote the source and the destination nodes, respectively; b_r denotes the requested bandwidth, represented in the number of FS; t_s and t_d are the requested setup and tear-down times, respectively. Therefore, the allocated spectrum bandwidth $B_{\text{allocated}}$ for service r (s, d, b_r, t_s, t_d) equals b_r, and the corresponding holding time $T_{\text{allocated}}$ equals the requested duration $(t_d–t_s)$ of the service connection. As for the fragmented spectrum consumption, the fragmented spectrum bandwidth B_{fragment} equals the isolated FS bands that contain no enough contiguous FSs for any kind of service connections, but the calculation of the corresponding holding time T_{fragment} is different from $T_{\text{allocated}}$ in this model. $T_{\text{allocated}}$ of the allocated spectrum equals the holding time of its served service connection, while T_{fragment} of the fragmented spectrum depends on the $T_{\text{allocated}}$ of its adjacent spectrum. By assuming the spectra adjacent to two sides of a fragmented spectrum being allocated to service request A $(s_A, d_A, b_{rA}, t_{sA}, t_{dA})$ and service request B $(s_B, d_B, b_{rB}, t_{sB}, t_{dB})$, T_{fragment} of the fragmented spectrum can be calculated as

$$T_{\text{fragment}} = \begin{cases} t_{dA} - t_{sB}, & t_{sA} < t_{sB} < t_{dA} < t_{dB} \\ t_{dB} - t_{sB}, & t_{sA} < t_{sB} < t_{dB} < t_{dA} \\ t_{dB} - t_{sA}, & t_{sB} < t_{sA} < t_{dB} < t_{dA} \\ t_{dA} - t_{sA}, & t_{sB} < t_{sA} < t_{dA} < t_{dB} \\ 0, & \text{others} \end{cases} \tag{2}$$

where t_{sA} and t_{dA} are the requested setup and tear-down times of service request A, respectively, while t_{sB} and t_{dB} are the requested setup and tear-down times of service request B, respectively.

3. ILP formulation for the RSA problem with time-scheduled traffic

In static traffic scenario, all connection requests with their setup and tear-down times are known in advance, which is similar to the time-scheduled traffic model in [32,33]. Therefore, a traffic model with scheduled time is adopted in the ILP formulation to minimize the comprehensive spectrum consumption in static traffic scenario. In the formulation, a network topology is represented by an undirected graph $\boldsymbol{G} = (\boldsymbol{V},\boldsymbol{E})$, where $\boldsymbol{V}$ denotes the set of nodes and $\boldsymbol{E}$ represents the set of undirected fiber links. $\boldsymbol{F}$ is assumed as the set of FSs on each fiber link, where FS is defined as the spectrum allocation granularity in EONs. The set of all service connection requests is denoted by $\boldsymbol{R}$ and each connection request is represented by $r(s, d, b_r, t_s, t_d)$. In the formulation, the durations of all connection requests are divided into a set of time slots $\boldsymbol{T}$, in which each time slot is represented by T_a, $a \in \{1, 2, 3 \ldots\}$. For example, we suppose that there are two service requests: r_1 with the setup time 01:00 and tear-down time 04:00, and r_2 with the setup time 03:00 and tear-down time 05:00. Then the time is divided into three time slots: T_1 (01:00–03:00), T_2 (03:00–04:00), and T_3 (04:00–05:00). Thus the holding time of r_1 can be expressed as $T_1 + T_2$, and the holding time of r_2 can be expressed as $T_2 + T_3$. Noticeably, each time slot T_a, $a \in \{1, 2, 3 \ldots\}$ in $\boldsymbol{T}$ are unnecessarily to be the same.

The variables of the ILP are listed as follows:

$L_{mn}^{r,T_a} \in \{0, 1\}$ – equal to 1 if request r is routed through the fiber link $e(m,n)$ in time slot T_a, and equal to 0 otherwise.
$X_{mn,f}^{r,T_a} \in \{0, 1\}$ – equal to 1 if the frequency slot f on the fiber link $e(m,n)$ is the FS with the lowest index in the spectrum band that serves connection request r in time slot T_a, and equal to 0 otherwise.
$Y_{mn,f}^{r,T_a} \in \{0, 1\}$ – equal to 1 if the frequency slot f on the fiber link $e(m,n)$ is one FS without the lowest index in the spectrum band that serves connection request r in time slot T_a, and equal to 0 otherwise.
$S_{mn,f}^{T_a} \in \{0, 1\}$ – equal to 1 if the frequency slot f on the fiber link $e(m,n)$ is the FS with the lowest index in a fragmented spectrum band in time slot T_a, and equal to 0 otherwise.
$P_{mn,f}^{T_a} \in \{0, 1\}$ – equal to 1 if the frequency slot f on the fiber link $e(m,n)$ is one FS without the lowest index in a fragmented spectrum band in time slot T_a, and equal to 0 otherwise.

The objective of the ILP is to minimize the comprehensive spectrum consumption which is comprised of the allocated and the fragmented spectrum consumptions:

$$\sum_{T_a \in T} \left\{ \sum_{mn \in E} \sum_{r \in R} L_{mn}^{r,T_a} \times b_r + \sum_{mn \in E} \sum_{f \in F} \left(S_{mn,f}^{T_a} + P_{mn,f}^{T_a} \right) \right\} \times |T_a| \tag{3}$$

Subject to

Routing path selection constraints:

$$\sum_{n \in V} L_{sn}^{r,T_a} = 1, \quad \forall r, T_a \text{ in the duration of } r \tag{4}$$

$$\sum_{m \in V} L_{md}^{r,T_a} = 1, \quad \forall r, T_a \text{ in the duration of } r \tag{5}$$

Equations (4) and (5) are the lightpath routing equations at the source and the destination nodes of service request r, respectively. They ensure that each service request selects a single routing path. s and d are the source and the destination nodes of the service request r, respectively.

$$\sum_{m \in V} L_{mk}^{r,T_a} = \sum_{n \in V} L_{kn}^{r,T_a}, \quad \forall r, T_a, k \neq s \text{ or } d \text{ of } r \tag{6}$$

Equation (6) ensures that if a service request goes through an intermediate node, it would go in and out the intermediate node only once.

$$L_{ij}^{r,T_a} = L_{ij}^{r,T_b}, \quad \text{if } T_a \text{ and } T_b \text{ are both in the duration of } r \tag{7}$$

Equation (7) ensures that the selected routing path cannot be changed during the holding time of r.

Spectrum allocation constraints:

$$\sum_{r \in R} L_{mn}^{r,T_a} \times b_r + \sum_{f \in F} \left(S_{mn,f}^{T_a} + P_{mn,f}^{T_a} \right) \leqslant |F|, \quad \forall m, n, T_a \tag{8}$$

Equation (8) ensures that the allocated spectrum and generated fragments on each link are less than the total spectrum resource on the link.

$$\sum_{r\in R}\left(X^{r,T_a}_{mn,f}+Y^{r,T_a}_{mn,f}\right)+S^{T_a}_{mn,f}+P^{T_a}_{mn,f}\leqslant 1,\quad \forall m,n,T_a \tag{9}$$

Equation (9) ensures that a FS on a link can never be allocated and fragmented simultaneously.

$$\left(L^{r,T_a}_{mn}-1\right)\times B+b_r\leqslant \sum_{f\in F}\left(X^{r,T_a}_{mn,f}+Y^{r,T_a}_{mn,f}\right)\leqslant b_r,\quad \forall m,n,r,T_a \tag{10}$$

$$\sum_{f\in F}\left(X^{r,T_a}_{mn,f}+Y^{r,T_a}_{mn,f}\right)\leqslant L^{r,T_a}_{mn}\times B,\quad \forall m,n,r,T_a \tag{11}$$

Equations (10) and (11) ensure that if a fiber link belongs to the routing path of request r, b_r FSs on the link are assigned to r, otherwise, none of the FSs on the link is assigned to r. b_r is the bandwidth (in number of FSs) of r. B is set to be a large value as in [34], which is much larger than other variables in the equations.

$$\left(X^{r,T_a}_{mn,f}-1\right)\times B+(b_r-1)\leqslant \sum_{f'\in[f+1,f+b_r-1]} Y^{r,T_a}_{mn,f'}\leqslant (b_r-1),\quad \forall m,n,r,T_a \tag{12}$$

Equation (12) ensures that the FSs assigned to the same request must be contiguous.

Spectrum fragmentation constraints:

$$\sum_{f'\in[Min(f+1,|F|),Min(f+Min(b),|F|)]} S^{T_a}_{mn,f'}\leqslant\left(1-S^{T_a}_{mn,f}\right)\times B,\quad \forall m,n,T_a \tag{13}$$

Equation (13) ensures that there is only one lowest indexed FS in one fragmented spectrum band, where $Min(b)$ represents the minimum bandwidth request among all service requests.

$$\left(S^{T_a}_{mn,f}-1\right)\times B+1\leqslant \sum_{f'\in[f+1,f+Min(b)]}\sum_{r\in R} X^{r,T_a}_{mn,f'}\leqslant 1,\quad \forall m,n,T_a \tag{14}$$

$$\left(2-S^{T_a}_{mn,f}-\sum_{r} X^{r,T_a}_{mn,f+I}\right)\times B+\sum_{f'\in[f+1,f+I-1]} P^{T_a}_{mn,f'}\geqslant I-1,$$
$$\forall m,n,T_a,\ I\in[2,Min(b)-1] \tag{15}$$

Equations (14) and (15) ensure that the maximum size of a fragmented spectrum band is $Min(b)-1$.

$$\sum_{f'\in[f+1,f+b_r-1]}\left\{\sum_{\bar r\in R,\bar r\neq r}\left(X^{\bar r,T_a}_{mn,f'}+Y^{\bar r,T_a}_{mn,f'}\right)+S^{T_a}_{mn,f'}+P^{T_a}_{mn,f'}\right\}$$
$$\leqslant\left(1-X^{r,T_a}_{mn,f}\right)\times B,\quad \forall m,n,r,T_a \tag{16}$$

Equation (16) ensures that if b_r FSs are assigned to request r, these FSs are occupied and can neither be marked as fragments nor be assigned to other service requests within the holding time of request r.

Since the RSA optimization problem in EONs is NP-complete whose difficulty mainly comes from the huge number of optimization variables in a large network [35], a small network with six nodes as shown in Fig. 1 is employed to illustrate the correctness of the formulation. In the illustration, each link in the network carries twelve FSs ($FS_0 \sim FS_{11}$) and there are totally four service connection requests: r_1 (A, D, 4, 00:00, 04:00), r_2 (D, E, 12, 00:00, 03:00), r_3 (A, E, 7, 00:00, 02:00), and r_4 (C, D, 7, 02:00, 04:00). According to the setup and tear-down times of the four service connections, we divide the time into three time slots: T_1 (00:00–02:00), T_2 (02:00–03:00), and T_3 (03:00–04:00). We also set the large number B as 99,999. After solving the ILP, four lightpaths have been established and the spectrum resource on each lightpath

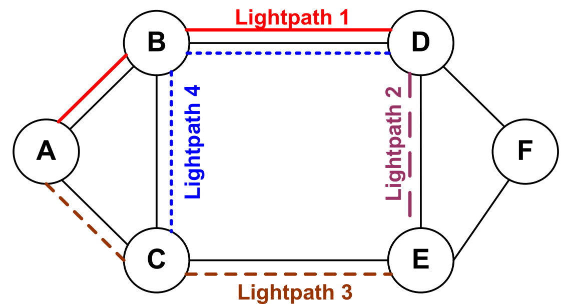

Fig. 1. Established lightpaths in the illustrative example.

has been allocated to the four service connections as shown in Fig. 1: lightpath 1 serves r_1 with the FSs from FS_0 to FS_3; lightpath 2 serves r_2 with the FSs from FS_0 to FS_{11}; lightpath 3 serves r_3 with the FSs from FS_0 to FS_6; and lightpath 4 serves r_4 with the FSs from FS_4 to FS_{10}. The comprehensive spectrum consumption C_{total} for the four service connection requests is 126, which includes both the allocated and fragmented spectrum consumptions. Although ILP formulation can be solved in small networks, it cannot be solved efficiently in large networks.

4. Spectrum efficient time-aware routing and spectrum assignment algorithm

In reality, optical networks always have quite large scale, such as NSFNET and USNET, which makes solving RSA optimization problem a calculation burden, when ILP formulation is calculated to seek the optimal routing and spectrum assignment strategy. What is more, service connections in reality are always set up dynamically and their setup and tear-down times cannot be predicted in advance. Therefore ILP formulation is no longer suitable for the RSA problem in reality with dynamic traffic. Instead, heuristic RSA algorithms are designed to solve the comprehensive spectrum consumption model in realistic dynamic traffic scenario, in which service connection requests arrive randomly and cannot be predicted in advance. In this paper, by employing the comprehensive spectrum consumption model, we propose a heuristic RSA algorithm, namely spectrum efficient time-aware routing and spectrum assignment (SETA-RSA) algorithm, to minimize the comprehensive spectrum consumption, C_{total}, in dynamic traffic scenario. However, considering the random traffic in dynamic scenario, the definition of fragmented spectrum bandwidth, $B_{fragment}$, represented in section II, should be revised accordingly. We assume that there are $\boldsymbol{N}$ kinds of service connections accommodated by the network. And the ith kind of the service connection requires n_i (for $i = 1,2,\ldots,N$) FS with a serving probability of p_i (for $i = 1,2,\ldots,N$), which means when a service connection arrives, it has a probability of p_i to be the ith kind of service. Then we represent the fragmented spectrum bandwidth, $B_{fragment}$, of an isolated vacant spectrum band containing n contiguous FS as follows:

$$B_{fragment}=\sum_{i\in N} n\cdot p_i\cdot K_i \tag{17}$$

where K_i is a boolean variable which equals 1 when n is less than n_i, and equals 0 otherwise. Equation (17) implies that if an isolated vacant spectrum band cannot be used by a service, it should be calculated as spectrum fragments at a corresponding probability. Except for $B_{fragment}$, the other parameters (e.g. $T_{fragment}$, $B_{allocated}$, $T_{allocated}$) in the proposed comprehensive spectrum consumption model, have the same definitions in both static and dynamic scenarios. Then, by adopting the comprehensive spectrum consumption model in Section 2, the details of proposed SETA-RSA algorithm are illustrated in the following pseudo-codes. Noticeably, although there are some other algorithms considering the holding times of service connections [36–38], these previous algorithms are quite different from the proposed SETA-RSA algorithm. For instance, the holding times of service connection in [36] were considered to optimize the consumed energy in wavelength routing networks. In [37,38], holding-times of connections were considered mainly for initial-delay-tolerant services (known as advance reservation service requests) to either optimize networking performance (e.g. blocking performance) [37] or minimize the generated spectrum fragments [38]. None of these algorithms have simultaneously optimized both the allocated and fragmented spectrum consumptions via holding times of service connections. In addition, since the algorithms in [37,38], are designed for advance reservation service requests, "how long should services be delayed" is one important issue in these algorithms and thus service start time should be carefully investigated. By comparison, our proposed algorithm is not specifically designed for advance reservation service requests, and thus service start time is not investigated in the algorithm, which reduces the complexity of the algorithm.

The complexity of the proposed spectrum efficient time-aware RSA algorithm is mainly determined by the adopted routing and spectrum assignment strategies. By adopting Dijkstra algorithm, the time complexity for finding the first K shortest paths for each s–d node pairs is $O(K \times |E| \times |V|^2)$, where $|E|$ is the number of edges in the network, $|V|$ is the number of nodes in the network. Since the construction of the solution set L for a service request is the main procedure in the spectrum assignment, the time complexity of assigning spectrum to a service request is $O(K \times |E| \times |F| \times B_{max} \times N)$, where $|F|$ is the number of FSs on a path, B_{max} is the maximum bandwidth request of a service connection, and N is the number of service kinds accommodated by the network. In general, the time complexity of the proposed algorithm is polynomial.

Algorithm 1 SETA-RSA algorithm

```
Pre-compute K shortest paths for each s–d node pairs
while network is running do
  When a request r(s, d, b_r, t_s, t_d) arrives, load the pre-computed paths set P for node pair s–d
  Make an empty routing and spectrum assignment solution set L to record the path, the allocated spectrum, and the spectrum consumption information for r
  for each path p in P do
    for each slot f in the slot set F along p do
      Check the availability of the consecutive b_r slots from f
      if all the b_r slots from f are available then
        Calculate the additional comprehensive spectrum consumption C_total caused by the new service request r assuming the b_r slots are allocated to r
        Add p, f and C_total to L as an possible solution l
      end if
    end for
  end for
  Check the solution set L
  If L is non-empty then
    Found the solution l with minimum C_total in L
    Select the path and assignment the spectrum to r according to l
    Update the network
  else
    Block the request r
  end if
end while
```

5. Performance evaluation

In this section, numerical simulations have been performed to evaluate the effectiveness of the proposed SETA-RSA algorithm in two typical networks, 14-node NSFNET (Fig. 2) and 24-node USNET (Fig. 3), when compared to two benchmarks, the typical K-shortest paths routing first-fit RSA algorithm without defragmentation [7] and the RSA algorithm employing spectrum defragmentation mechanism [10]. In the simulations, none of the network nodes have the capability of optical spectrum conversion, given its high cost and complexity in reality, and each link in the network consists of two unidirectional fibers with a total spectrum of 4000 GHz on each fiber. A spectrum of 12.5-GHz is employed as one FS. We also assume that there are three typical kinds of service connections accommodated by the network, namely 100-Gb/s, 400-Gb/s and 1 Tb/s. By employing QPSK, 16-QAM and 32-QAM as the modulation formats for 100-Gb/s, 400-Gb/s and 1 Tb/s service connections, respectively, the required bandwidths (including guard-band) of the three kinds of service connections are 50-GHz, 80-GHz [39], 150-GHz [40], respectively. Therefore, the three kinds of service connections require 4 FSs, 7 FSs and 12 FSs, respectively, and the proportion of the three kinds of service connections is set as 1:1:1. All the service connections are generated dynamically employing the Poisson traffic model with parameter λ and their respective duration satisfies negative exponential distribution with parameter μ. Hence, the traffic load is calculated as λ/μ Erlang. The kind of each service connection is randomly generated among the three kinds, and the source and destination nodes of each service connection are also randomly generated among all node pairs in the network.

In the simulations, we investigate the average allocated spectrum consumption (AASC) and the average fragmented spectrum consumption (AFSC), as well as the bandwidth blocking probability (BBP) of the proposed algorithm with different value of K, where K is the number of pre-computed shortest paths for each node pair. In the numerical evaluation, AASC is defined as the average product of $B_{allocated}$ and $T_{allocated}$ for each service connection, AFSC is defined as the average product of $B_{fragment}$ and $T_{fragment}$ for each service connection, and BBP is the ratio of the blocked bandwidth to all the requested bandwidth. Noticeably, both blocked bandwidth and requested bandwidth are represented in FS in the simulations.

5.1. NSFNET

Fig. 4 shows the average allocated spectrum consumption over different traffic loads in NSFNET with different value of K, when the proposed SETA RSA algorithm, the typical first-fit RSA algorithm [7], and the defragmentation algorithm [10] are employed. As

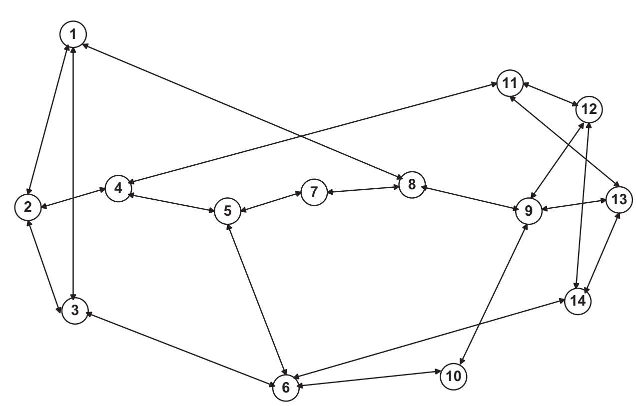

Fig. 2. 14-node NSFNET.

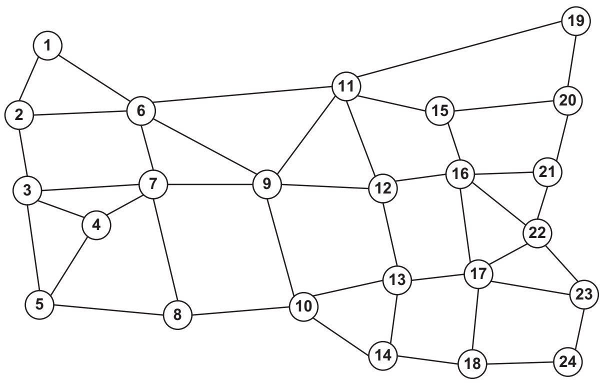

Fig. 3. 24-node USNET.

shown in Fig. 4(a), when three shortest paths are pre-computed in the simulation, the proposed SETA RSA algorithm exhibits similar average allocated spectrum consumption compared to the typical first-fit RSA algorithm without defragmentation mechanism, but exhibits lower average allocated spectrum consumption than the defragmentation algorithm. This may be mainly induced by the defragmentation procedure, which may lengthen the routing path and require more allocated spectrum during rerouting the existing service connections. Fig. 4(b) depicts the average allocation spectrum consumption, when six shortest paths are pre-computed in the simulation. Although more candidate paths are pre-computed, the simulation results are similar to those in Fig. 4(a), which implies that increasing the value of K may not obviously affect the average allocated spectrum consumption in NSFNET.

Fig. 5 shows the average fragmented spectrum consumption over different traffic loads in NSFNET with different value of K, when the proposed SETA RSA algorithm, the typical first-fit RSA algorithm, and the defragmentation algorithm are employed. As shown in Fig. 5(a), with three pre-computed shortest paths, the proposed SETA RSA algorithm can effectively reduce more than 91% fragmented spectrum consumption with low traffic load (e.g. 100 Erlang) and more than 44% with high traffic load (e.g. 500 Erlang), compared to the typical first-fit RSA algorithm. Fig. 5(a) also depicts that the proposed SETA RSA algorithm displays lower average fragmented spectrum consumption than the defragmentation algorithm when the traffic load is higher than 350 Erlang, which verifies that the proposed algorithm can effectively reduce the fragmented spectrum consumption in spectrum assignment with no defragmentation mechanism. Fig. 5(b) shows the average fragmented spectrum consumption in NSFNET when six shortest paths are pre-computed in the simulation. Similar results can be observed in Fig. 5(b) compared with those in Fig. 5(a), except that the proposed SETA RSA algorithm displays lower average fragmented spectrum consumption than the defragmentation algorithm when the traffic load is higher than 300 Erlang, which implies that with more candidate paths the proposed algorithm may have less fragmented spectrum consumption than the defragmentation algorithm with lower traffic load.

Fig. 6 shows the bandwidth blocking probability over different traffic loads in NSFNET with different value of K, when the proposed SETA RSA algorithm, the typical first-fit RSA algorithm, and the defragmentation algorithm are employed. As shown in Fig. 6 (a), with three pre-computed shortest paths, the proposed SETA RSA algorithm has better bandwidth blocking performance than the typical first-fit RSA algorithm, but worse bandwidth blocking performance than the defragmentation algorithm. Nevertheless, the blocking performance difference between the proposed RSA algorithm and the defragmentation RSA algorithm decreases with the increase of traffic load. Noticeably, since there is no traffic disruption or any technique limitation in the proposed algorithm compared to the defragmentation algorithm, the proposed algorithm can be easily realized in reality. Fig. 6(b) shows the bandwidth blocking performance of the three algorithms in NSFNET with six shortest paths pre-computed in the simulation. Similar results can be observed in Fig. 6(b) compared to those in Fig. 6 (a), except that the bandwidth blocking probabilities of all the three algorithms decreases with the increased number of pre-computed shortest paths, which implies more candidate paths can reduce the bandwidth blocking probability.

5.2. USNET

Fig. 7 shows the average allocated spectrum consumption over different traffic loads with different value of K in a larger network, USNET, when the proposed SETA RSA algorithm, the typical first-fit RSA algorithm, and the defragmentation algorithm are employed. Similar to that in NSFNET, the proposed SETA RSA algorithm exhibits similar average allocated spectrum consumption compared to the typical first-fit RSA algorithm, but lower average allocated

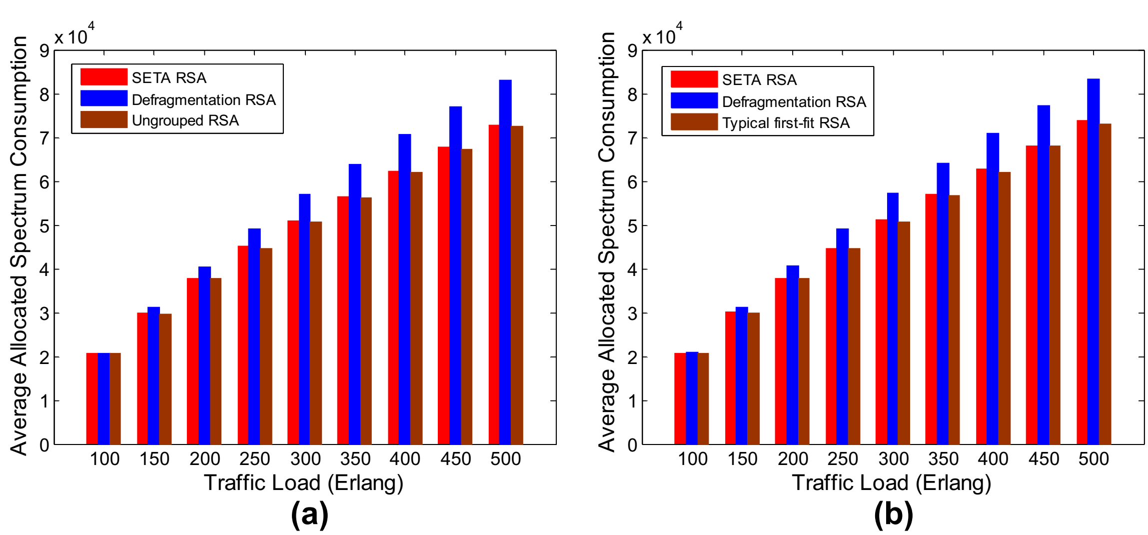

Fig. 4. *AASC* vs. traffic load in NSFNET with different value of K. (a) *AASC* vs. traffic load when $K = 3$; (b) *AASC* vs. traffic load when $K = 6$.

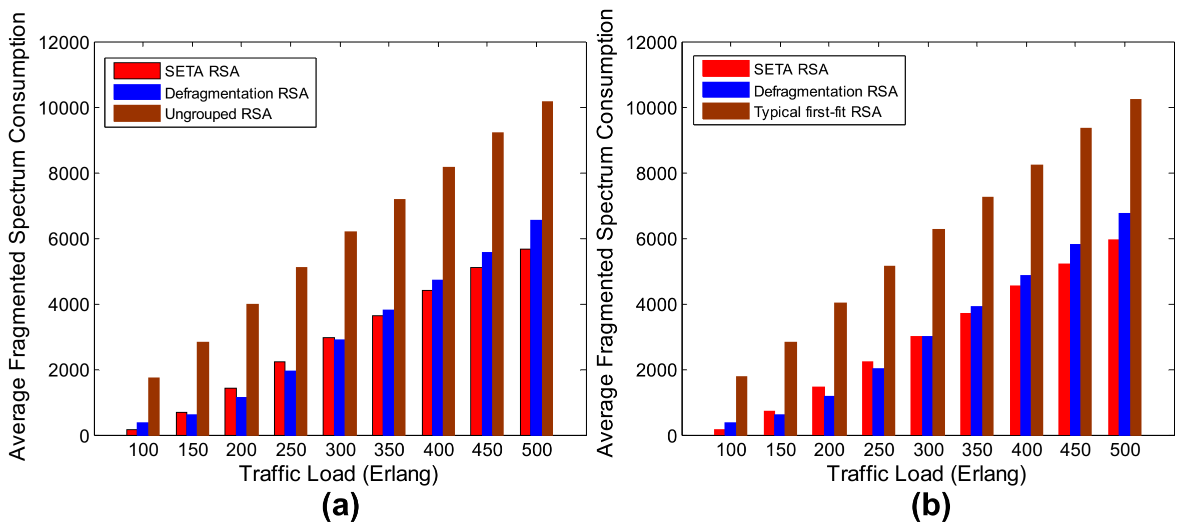

Fig. 5. *AFSC* vs. traffic load in NSFNET with different value of *K*. (a) *AFSC* vs. traffic load when $K = 3$; (b) *AFSC* vs. traffic load when $K = 6$.

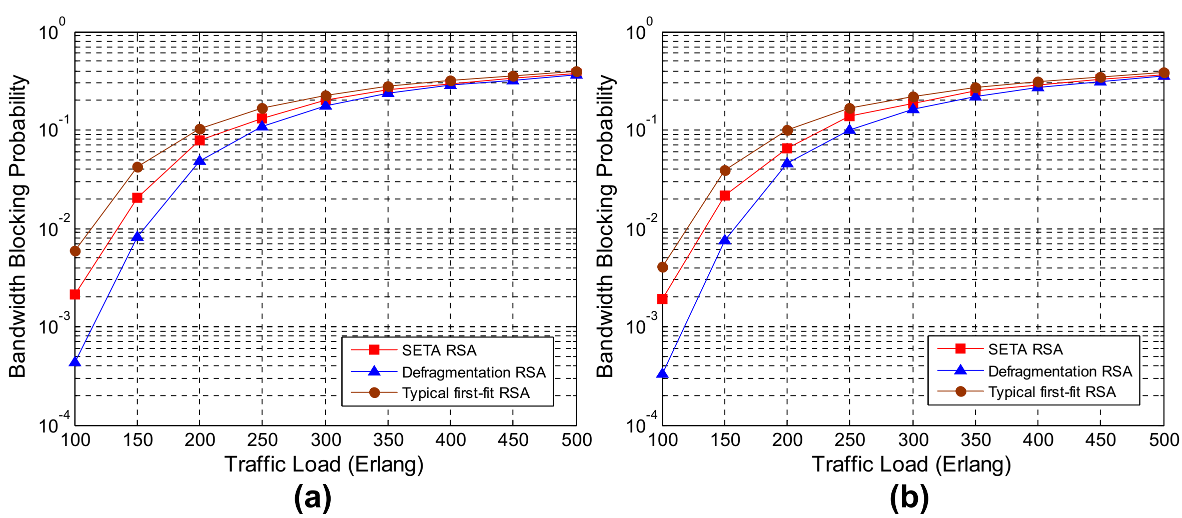

Fig. 6. *BBP* vs. traffic load in NSFNET with different value of *K*. (a) *BBP* vs. traffic load when $K = 3$; (b) *BBP* vs. traffic load when $K = 6$.

spectrum consumption than the defragmentation algorithm, with either three or six pre-computed shortest paths. Fig. 7(a) and (b) have similar results, which imply that even in a larger network increasing the value of *K* may not obviously affect the average allocated spectrum consumption.

Fig. 8 shows the average fragmented spectrum consumption over different traffic loads in USNET with different value of *K*, when the proposed SETA RSA algorithm, the typical first-fit RSA algorithm, and the defragmentation algorithm are employed. As shown in Fig. 8(a), with three pre-computed shortest paths, the proposed SETA RSA algorithm can effectively reduce more than 95% fragmented spectrum consumption with low traffic load (e.g. 100 Erlang) and more than 48% with high traffic load (e.g. 500 Erlang), compared to the typical first-fit RSA algorithm. Fig. 8(a) also depicts that the proposed SETA RSA algorithm displays lower average fragmented spectrum consumption than the defragmentation algorithm, which verifies that the proposed algorithm can effectively reduce the fragmented spectrum consumption in spectrum assignment with no defragmentation mechanism, especially in a larger network. Fig. 8(b) shows the average fragmented spectrum consumption in USNET when six shortest paths are pre-computed in the simulation. Similar results can be observed in Fig. 8(b) compared with those in Fig. 8(a), except that the fragmented spectrum consumptions of the three algorithms increases with the increased number of pre-computed shortest paths, which implies more candidate paths may possibly induce more fragmented spectrum, especially in a large network.

Fig. 9 shows the bandwidth blocking probability over different traffic loads in USNET with different value of *K*, when the proposed SETA RSA algorithm, the typical first-fit RSA algorithm, and the defragmentation algorithm are employed. Similar to that in NSFNET, the proposed SETA RSA algorithm has better bandwidth blocking performance than the typical first-fit RSA algorithm, but worse bandwidth blocking performance than the defragmentation algorithm with three pre-computed shortest paths as in Fig. 9(a). Nevertheless, the blocking performance difference between the proposed RSA algorithm and the defragmentation RSA algorithm decreases with the increase of traffic load. Fig. 9(b) shows the bandwidth blocking performance of the three algorithms in USNET with six shortest paths pre-computed in the simulation. Similar results can be observed in Fig. 9(b) compared to those in Fig. 9(a), except that the bandwidth blocking probabilities of all the

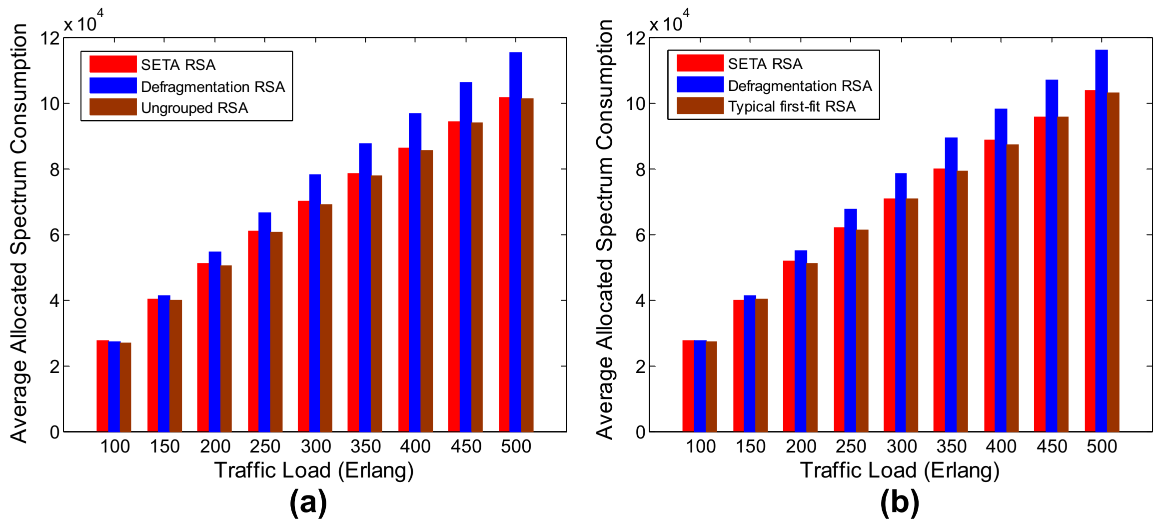

Fig. 7. *AASC* vs. traffic load in USNET with different value of *K*. (a) *AASC* vs. traffic load when $K = 3$; (b) *AASC* vs. traffic load when $K = 6$.

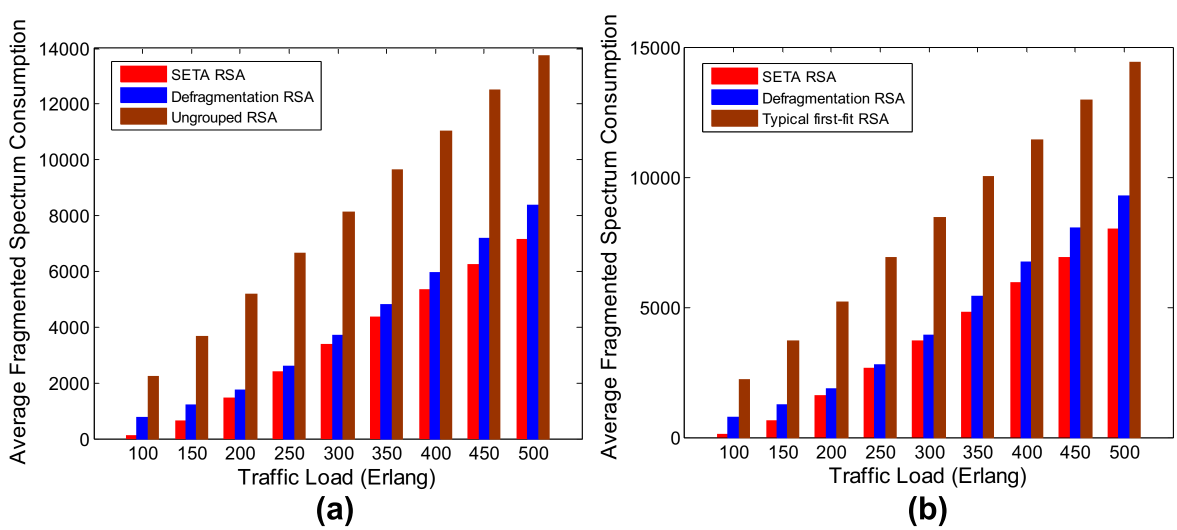

Fig. 8. *AFSC* vs. traffic load in USNET with different value of *K*. (a) *AFSC* vs. traffic load when $K = 3$; (b) *AFSC* vs. traffic load when $K = 6$.

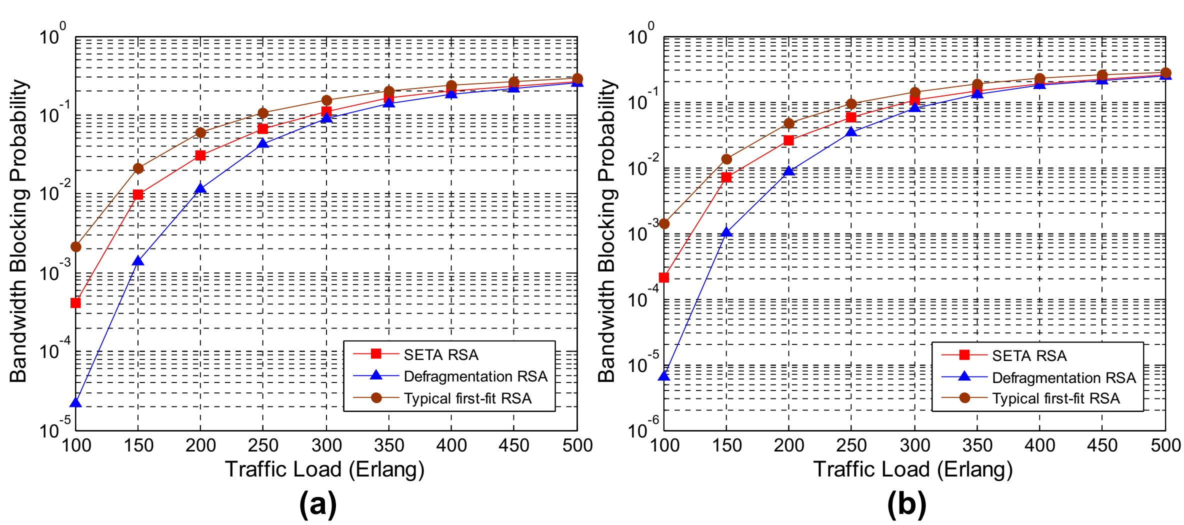

Fig. 9. *BBP* vs. traffic load in USNET with different value of *K*. (a) *BBP* vs. traffic load when $K = 3$; (b) *BBP* vs. traffic load when $K = 6$.

three algorithms decreases with the increased number of pre-computed shortest paths, which implies that more candidate paths can reduce the bandwidth blocking probability in a larger network.

6. Conclusion

In this paper, we investigated the comprehensive spectrum consumption, including both the allocated and the fragmented spectrum consumptions during the routing and spectrum assignment procedure in EONs. By additionally considering the holding times of the lightpaths and connection requests, we set up ILP formulation to analyze the allocated and the fragmented spectrum consumptions comprehensively in static scenario and proposed a spectrum efficient routing and spectrum assignment algorithm, SETA RSA algorithm, to simultaneously optimize the allocated and the fragmented spectrum consumptions in dynamic scenario. Numerical simulations have also been set up to verify the effectiveness of proposed SETA RSA algorithm. The simulation results show that the proposed RSA algorithm reduces the spectrum consumption with no traffic disruption and has better bandwidth blocking performance than the typical first-fit RSA algorithm.

Acknowledgments

This work was partly supported by the Fundamental Research Funds for the Central Universities, Southwest University for Nationalities (Project No. 13NZYBS04), Sichuan Provincial Science and technology project (Project No. 2014GZ0015), and Sichuan Provincial Department of education project (Project No. 15TD0050). We appreciate the reviewers' suggestions on the paper.

References

[1] M. Jinno, H. Takara, B. Kozicki, Y. Tsukishima, Y. Sone, S. Matsuoka, Spectrum-efficient and scalable elastic optical path network: architecture, benefits, and enabling technologies, IEEE Commun. Mag. 47 (11) (2009) 66–73.
[2] ITU-T Recommendation G.694.1, June 2002.
[3] L. Guo, W. Hou, J. Wu, Y. Li, Multicast multi-granular grooming based on integrated auxiliary grooming graph in optical networks, Photonic Network Commun. 24 (2) (2012) 103–117.
[4] Y. Wang, X. Cao, Multi-granular optical switching: a classified overview for the past and future, IEEE Commun. Surv. Tutorials 14 (3) (2012) 698–713.
[5] S. Frisken, G. Baxter, D. Abakoumov, H. Zhou, I. Clarke, S. Poole, Flexible and grid-less wavelength selective switch using LCOS technology, in: IEEE/OSA OFC/NFOEC, Paper OTuM3, 2011.
[6] K. Christodoulopoulos, I. Tomkos, E. Varvarigos, Elastic bandwidth allocation in flexible OFDM-based optical networks, J. Lightwave Technol. 29 (9) (2011) 1354–1366.
[7] W. Zheng et al., On the spectrum efficiency of bandwidth-variable optical OFDM transport networks, 2010. OFC, 1–3.
[8] M. Jinno, B. Kozicki, H. Takara, A. Watanabe, Y. Sone, T. Tanaka, A. Hirano, Distance-adaptive spectrum resource allocation in spectrum-sliced elastic optical path network, IEEE Commun. Mag. 48 (8) (2010) 138–145.
[9] T. Takagi, H. Hasegawa, K. Sato1, Y. Sone, B. Kozicki, A. Hirano, M. Jinno, Dynamic routing and frequency slot assignment for elastic optical path networks that adopt distance adaptive modulation, in: IEEE/OSA OFC/NFOEC, Paper OTuI7, 2011.
[10] A.N. Patel, P.N. Ji, J.P. Jue, T. Wang, Defragmentation of transparent flexible optical WDM (FWDM) networks, in: IEEE/OSA OFC/NFOEC, Paper OTuI8, 2011.
[11] W. Shi, Z. Zhu, M. Zhang, N. Ansari, On the effect of bandwidth fragmentation on blocking probability in elastic optical networks, IEEE Trans. Commun. 61 (7) (2013) 2970–2978.
[12] T. Takagi, H. Hasegawa, K. Sato, Y. Sone, A. Hirano, M. Jinno, Disruption minimized spectrum defragmentation in elastic optical path networks that adopt distance adaptive modulation, in: Proc. Eur. Conf. Exhib. Opt. Commun., 2011, pp. 1–3.
[13] K. Christodoulopoulos, I. Tomkos, E. Varvarigos, Dynamic bandwidth allocation in flexible OFDM-based networks, in: Proc. Opt. Fiber Commun. Conf., 2011, pp. 1–3.
[14] E. Palkopoulou et al., Dnamic cooperative spectrum sharing in elastic networks, in: 2013 (Ed.), Proc. Opt. Fiber Commun. Conf., 2013, pp. 1–3.
[15] K. Christodoulopoulos, I. Tomkos, E. Varvarigos, Time-varying spectrum allocation policies and blocking analysis in flexible optical networks, IEEE J. Sel. Areas Commun. 31 (1) (2013) 13–25.
[16] M. Klinkowski, M. Ruiz, L. Velasco, D. Careglio, V. Lopez, J. Comellas, Elastic spectrum allocation for time-varying traffic in flexgrid optical networks, IEEE J. Sel. Areas Commun. 31 (1) (2013) 26–38.
[17] R. Wang, B. Mukherjee, Provisioning in elastic optical networks with non-disruptive defragmentation, J. Lightwave Technol. 31 (15) (2013) 2491–2500.
[18] M. Zhang, Y. Yin, R. Proietti, Z. Zhu, B. Yoo, Spectrum defragmentation algorithms for elastic optical networks using hitless spectrum retuning techniques, in: Proc. Opt. Fiber Commun. Conf., 2013, pp. 1–3.
[19] M. Zhang, W. Shi, L. Gong, W. Lu, Z. Zhu, Bandwidth defragmentation in dynamic elastic optical networks with minimum traffic disruptions, in: Proc. IEEE Int. Conf. Commun., 2013, pp. 3894–3898.
[20] Y. Yin, K. Wen, D. Geisler, R. Liu, B. Yoo, Dynamic on-demand defragmentation in flexible bandwidth elastic optical networks, Opt. Exp. 20 (2012) 1798–1804.
[21] S. Shakya, X. Cao, Spectral defragmentation in elastic optical path networks using independent sets, in: Proc. Opt. Fiber Commun. Conf., 2013, pp. 1–3.
[22] F. Cugini, F. Paolucci, G. Meloni, G. Berrettini, M. Secondini, F. Fresi, N. Sambo, L. Poti, P. Castoldi, Push–pull defragmentation without traffic disruption in flexible grid optical networks, J. Lightwave Technol. 31 (1) (2013) 125–133.
[23] Yawei Yin, Mingyang Zhang, Zuqing Zhu, S.J.B. Yoo, Fragmentation-aware routing, modulation and spectrum assignment algorithms in elastic optical networks, in: IEEE/OSA OFC/NFOEC, Paper OW3A.5, 2013.
[24] Tatsuya Fukuda, Lei Liu, Ken-ichi Baba, Shinji Shimojo, S.J.B. Yoo, Fragmentation aware spectrum assignment for elastic optical networks with fully-distributed GMPLS, in: IEEE/OSA OFC/NFOEC, Paper Tu2B.3, 2015.
[25] Antonio Napoli, Markus Nolle, Danish Rafique, Johannes K. Fischer, Bernhard Spinnler, Talha Rahman, Mahdi M. Mezghanni, Marc Bohn, On the next generation bandwidth variable transponders for future flexible optical systems, in: Eur. Conf. Networks Commun., 2014, pp. 1–5.
[26] N. Sambo, G. Meloni, F. Paolucci, F. Cugini, M. Secondini, F. Fresi, L. Poti, P. Castoldi, Programmable transponder, code and differentiated filter configuration in elastic optical networks, J. Lightwave Technol. 32 (11) (2014) 2079–2086.
[27] M.F. Huang, S. Zhang, E. Mateo, D. Qian, F. Yaman, T. Inoue, Y. Inada, T. Wang, EDFA-only WDM 4200-km transmission of OFDM-16QAM and 32QAM, IEEE Photonics Technol. Lett. 24 (17) (2012) 1466–1468.
[28] T. Kobayashi, A. Sano, A. Matsuura, Y. Miyamoto, K. Ishihara, Nonlinear tolerant long-haul WDM transmission over 1200 km using 538Gb/s/ch PDM-64QAM SC-FDM signals with pilot tone, in: IEEE/OSA OFC/NFOEC, Paper OM2A.5, 2012.
[29] X. Zhou, L.E. Nelson, R. Isaac, P.D. Magill, B. Zhu, D.W. Peckham, P. Borel, K. Carlson, 4000 km transmission of 50 GHz spaced, 10 × 494.85-Gb/s hybrid 32-64QAM using cascaded equalization and training-assisted phase recovery, in: IEEE/OSA OFC/NFOEC, Paper PDP5C.6, 2012.
[30] D. Chang, F. Yu, Z. Xiao, N. Stojanovic, F.N. Hauske, Y. Cai, C. Xie, L. Li, X. Xu, Q. Xiong, LDPC convolutional codes using layered decoding algorithm for high speed coherent optical transmission, in: IEEE/OSA OFC/NFOEC, Paper OW1H.4, 2012.
[31] S. Zhang, F. Yaman, Y. Huang, J.D. Downie, D. Zou, W.A. Wood, A. Zakharian, R. Khrapko, S. Mishra, V. Nazarov, J. Hurley, I.B. Djordjevic, E. Mateo, Y. Inada, Capacity-approaching transmission over 6375 km at spectral efficiency of 8.3 bit/s/Hz, in: IEEE/OSA OFC/NFOEC, Paper Th5C.2, 2016.
[32] T. Li, B. Wang, C. Xin, X. Zhang, On survivable service provisioning in WDM optical networks under a scheduled traffic model, in: Proc. IEEE Global Commun. Conf., 2005, pp. 1900–1904.
[33] S. Zhang, C.K. Chan, Multicast protection in WDM optical networks with scheduled traffic, in: Proc. Eur. Conf. Opt. Commun., 2009, pp. 1–2.
[34] Y. Wang, X. Cao, Y. Pan, A Study of the Routing and Spectrum Allocation in Spectrum-sliced Elastic Optical Path Networks, INFOCOM, 2011, pp. 1503–1511.
[35] M. Klinkowski, K. Walkowiak, Routing and spectrum assignment in spectrum sliced elastic optical path network, in: IEEE Commun. Lett., 2011, pp. 884–886.
[36] S. Zhang, D. Shen, C.K. Chan, Energy efficient time-aware traffic grooming in wavelength routing networks, in: Proc. IEEE Global Commun. Conf., 2010, pp. 1–5.
[37] Wei Lu, Zuqing Zhu, Dynamic service provisioning of advance reservation requests in elastic optical networks, J. Lightwave Technol. 31 (10) (2013) 1621–1627.
[38] Haoran Chen, Yongli Zhao, Jie Zhang, Ruiying He, Wei Wang, Jialin Wu, Yike Wang, Yuefeng Ji, Haomian Zheng, Yi Lin, Baogang Hou, Time-spectrum consecutiveness based scheduling with advance reservation in elastic optical networks, Commun. Lett. (2015) 70–73.
[39] Kim Roberts, Ian Roberts, DSP: a disruptive technology for optical transceivers, in: IEEE ECOC, Paper 4.4.2, 2009.
[40] S. Gringeri, B. Basch, V. Shukla, R. Egorov, T.J. Xia, V. Laboratories, Flexible architectures for optical transport nodes and networks, IEEE Commun. Mag. 48 (7) (2010) 40–50.